Dynamic 3D Compressed Sensing MR of hyperpolarized 13C Pyruvate and Urea in Prostate Cancer Models

Hsin-Yu Chen[1], Peder E. Z. Larson[2], Cornelius von Morze[2], Christine Leon Swisher[1], Naeim Bahrami[2], Robert Bok[2], John Kurhanewicz[1,2], and Daniel B. Vigneron[1,2]
[1]*Graduate Program in Bioengineering, UCSF and UC Berkeley, San Francisco, California, United States,* [2]*Department of Radiology and Biomedical Imaging, University of California, San Francisco, California, United States*

Target Audience: Researchers interested in preclinical cancer imaging and hyperpolarized ^{13}C imaging.

Purpose: Prostate cancer has the highest incidence of all non-cutaneous malignancies in men and degrades patient quality of life in the U.S.[1]. Unfortunately, no existing prognostic marker confidently discriminates between aggressive and indolent forms. In this study, we developed novel methods for 3D dynamic MRSI of co-hyperpolarized [1-^{13}C]pyruvate and [^{13}C]urea to provide simultaneous measures of metabolism and perfusion using a preclinical prostate tumor model. In prostate cancer, the increased metabolic conversion from pyruvate to lactate correlates with its aggressiveness[2]. Altered vasculature and perfusion also characterize tumor progression. Rapid acquisition of 3D dynamic data was achieved by a MRSI sequence applying multiband excitation and compressed sensing for high spatiotemporal resolution. Dynamic modeling was used to calculate metabolic and perfusion parameters k_{pl} and k_{trans}.

Methods: Pulse Sequence: A 3D dynamic MRSI sequence was designed to capture the metabolic and perfusion patterns[3]. Spectral-spatial RF excitation was followed by double spin-echo refocusing and EPSI readout with random blips. (spectral BW= 581Hz, spectral res= 9.83Hz, FOV=4x4x8.6cm^3, res= 3.3x3.3x5.4mm^3) Multiband variable-flip excitation was applied to efficiently utilize magnetization. To start, pyruvate is excited with smaller flip angles than lactate and alanine, which effectively preserves pyruvate hyperpolarization to maintain high lactate and alanine SNR throughout the entire acquisition. A progressively increasing flip angle compensates for loss of magnetization due to each excitation pulse. Compressed sensing using in-plane random encoding enables a rapid time-series acquisition in 36s with 2s time resolution. The EPSI spectral bandwidth allows for simultaneous pyruvate, lactate, urea and alanine detection. We also found that limiting the acquisition length ensures good SNR.

Metabolic exchange: Tumor tissue exhibits elevated conversion from pyruvate to lactate. Conversion between pyruvate and lactate was modeled as $\frac{dC_{lac}(t)}{dt} = k_{pl}C_{pyr}(t) - k_{lp}C_{lac}(t)$, where $C_{species}(t)$ is the metabolite concentration, and k_{pl} and k_{lp} are the forward and the reverse conversion rate, respectively. Conversion between pyruvate and alanine was modeled in much the same way. T_1 relaxation was assumed to be equal for all metabolites, and a correction was incorporated to account for the multiband excitation and variable flip angles. A nonlinear least-square fitting was performed, giving estimates of k_{pl} and k_{pa}, where reverse conversion rates were assumed to be zero.

Perfusion modeling: Tumor microcirculation can be characterized by the perfusion and permeability between blood and tissue[4]. A model-based arterial input function (AIF) defined by a gamma-variate function was employed to model the infusion of [^{13}C]urea[5]. Perfusion dynamics can be described as $\frac{dC_{tissue}(t)}{dt} = k_{trans}C_{blood}(t) - k_{ep}C_{tissue}(t)$, where $C_{blood}(t)$ is the AIF, $C_{tissue}(t)$ is the concentration in tissue, $k_{trans}\ (ml/dL \cdot min^{-1})$ and $k_{ep}(min^{-1})$ are forward and backward perfusion rate, respectively. Nonlinear fitting was applied to the urea dynamics from both aorta and tumor tissue with correction for flip angle and T1 relaxation, yielding estimates of k_{trans} and k_{ep}.

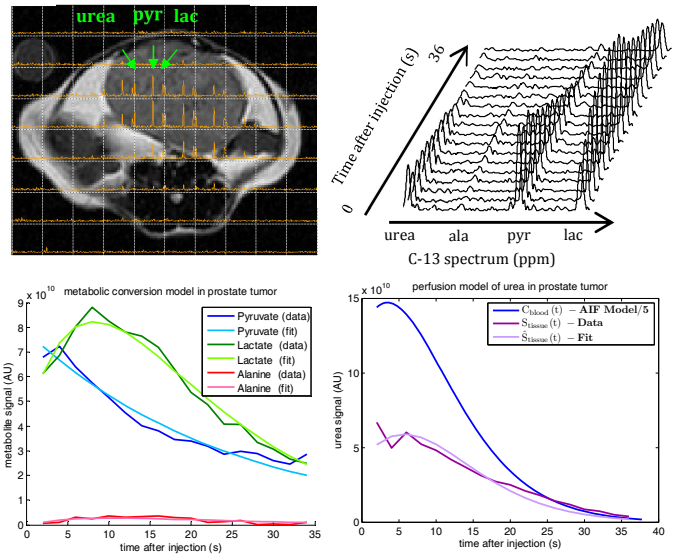

Fig 1 (Top left) High spatiotemporal resolution is achieved with the 3D dynamic variable-flip sequence. (Top right) The spectral-time plot depicts increased pyruvate to lactate conversion in prostate tumor. Note that lactate and urea are aliased in the spectrum (Bottom) Fitting between data and metabolic-perfusion models shows good agreement.

Hyperpolarization and Imaging Experiments: In this project, transgenic mice (N=6) with prostate cancer (TRAMP model[7]) were studied. [^{13}C]Pyruvate and [^{13}C]urea were co-polarized by a 3.35T clinical polarizer in development[6]. 350ul of 80mM concentration of co-polarized pyruvate and urea (30~40% polarization) were administered over 15 seconds through tail vein and the image acquisition started at the end of injection.

Results and Discussion: The 3D dynamic ^{13}C data quantitatively measures *in vivo* pyruvate-to-lactate conversion and urea uptake in prostate tumors. This specialized sequence provided optimized SNR for high spatiotemporal analysis. Both metabolic and perfusion levels were elevated in the prostate tumors ($k_{pl} = 0.0389, k_{pa} = 0.0014, k_{trans} = 365\ ml/dL \cdot min^{-1}$) versus normal tissue, consistent with previous studies[8,9]. The number and range of model variables were carefully chosen to minimize the Akaike's information criterion (AIC)[10], such that the model is well-determined and the fitting stability can be assured. This was validated by the good agreement between dynamic data and models, in addition to the spatially-coherent k_{pl} and k_{trans} estimates in the MRSI data.

Conclusion: Use of 3D compressed-sensing [^{13}C]pyruvate and [^{13}C]urea MRSI sequence and dynamic models enables, for the first time, simultaneous evaluation of metabolic and perfusion parameters k_{pl} and k_{trans} in a preclinical prostate tumor model. The data demonstrates increases in both pyruvate-to-lactate conversion rate and perfusion/permeability in prostate tumor versus normal tissue. This approach shows great potential for the quantitative assessment of prostate cancer aggressiveness and also treatment response.

Acknowledgement: This work was supported by grants from the NIH and the DOD Prostate Cancer Research Program.

References- [1] ACS. 2012. [2] Kurhanewicz et al. Neoplasia. 2012. [3] Xing et al. JMR. 2013. [4] de Langen et al. Onc. 2008. [5] von Morze et al. JMRI. 2011. [6] Hu et al. MRM. 2012. [7] Hurwitz et al. C P Immunology. 2001. [8] Zierhut et al. JMR. 2010. [9] Harrison et al. NMR Biomed. 2012. [10] Akaike et al. IEEE T. Automat. Contr. 1974.